

# Generation of a patient-derived chordoma xenograft and characterization of the phosphoproteome in a recurrent chordoma

## Laboratory investigation

JASON M. DAVIES, M.D., PH.D.,<sup>1</sup> AARON E. ROBINSON, B.Sc.,<sup>1,2</sup> CYNTHIA COWDREY,<sup>1,2</sup>  
PRAVEEN V. MUMMANENI, M.D.,<sup>1</sup> GREGORY S. DUCKER, PH.D.,<sup>4</sup> KEVAN M. SHOKAT, PH.D.,<sup>4</sup>  
ANDREW BOLLEN, M.D., D.V.M.,<sup>2,3</sup> BYRON HANN, M.D., PH.D.,<sup>5</sup>  
AND JOANNA J. PHILLIPS, M.D., PH.D.<sup>1-3</sup>

<sup>1</sup>Department of Neurological Surgery, <sup>2</sup>Brain Tumor Research Center, <sup>3</sup>Department of Pathology,  
<sup>4</sup>Department of Cellular and Molecular Pharmacology and Howard Hughes Medical Institute, and <sup>5</sup>UCSF  
Helen Diller Family Comprehensive Cancer Center, University of California, San Francisco, California

**Object.** The management of patients with locally recurrent or metastatic chordoma is a challenge. Preclinical disease models would greatly accelerate the development of novel therapeutic options for chordoma. The authors sought to establish and characterize a primary xenograft model for chordoma that faithfully recapitulates the molecular features of human chordoma.

**Methods.** Chordoma tissue from a recurrent clival tumor was obtained at the time of surgery and implanted subcutaneously into NOD-SCID interleukin-2 receptor gamma (IL-2R $\gamma$ ) null (NSG) mouse hosts. Successful xenografts were established and passaged in the NSG mice. The recurrent chordoma and the derived human chordoma xenograft were compared by histology, immunohistochemistry, and phospho-specific immunohistochemistry. Based on these results, mice harboring subcutaneous chordoma xenografts were treated with the mTOR inhibitor MLN0128, and tumors were subjected to phosphoproteome profiling using Luminex technology and immunohistochemistry.

**Results.** SF8894 is a novel chordoma xenograft established from a recurrent clival chordoma that faithfully recapitulates the histopathological, immunohistological, and phosphoproteomic features of the human tumor. The PI3K/Akt/mTOR pathway was activated, as evidenced by diffuse immunopositivity for phospho-epitopes, in the recurrent chordoma and in the established xenograft. Treatment of mice harboring chordoma xenografts with MLN0128 resulted in decreased activity of the PI3K/Akt/mTOR signaling pathway as indicated by decreased phospho-mTOR levels ( $p = 0.019$ ,  $n = 3$  tumors per group).

**Conclusions.** The authors report the establishment of SF8894, a recurrent clival chordoma xenograft that mimics many of the features of the original tumor and that should be a useful preclinical model for recurrent chordoma. (<http://thejns.org/doi/abs/10.3171/2013.10.JNS13598>)

**KEY WORDS** • chordoma xenograft • SF8894 • mTOR • phosphoproteome • oncology

**C**HORDOMA is a malignant tumor that arises predominantly in the axial skeleton, with the base of skull and the distal spine being the most common sites of disease. Chordomas are often slow-growing tumors treated by resection and adjuvant proton-beam radiation therapy.<sup>22</sup> Despite their typical lower-grade features, chordomas have a relatively high recurrence rate. This is thought to be a consequence of a combination of factors, including the proximity of tumors to vital structures, complicating their resection and the relative resistance of tumor cells to radiotherapy and chemotherapy.<sup>2</sup> Although recent studies suggest targeted therapeutics may have antitumor activity in some patients, the clinical benefits of

these therapies have so far been modest.<sup>12,30</sup> Additional therapeutic strategies are clearly needed.

Identifying therapeutic targets in chordoma has been challenging, but a consensus is emerging that significant receptor tyrosine kinase (RTK) overexpression is common in tumors, albeit poorly conserved.<sup>19,28,32–34</sup> Consequently, downstream effectors of RTK signaling appear to be nearly uniformly activated in chordoma, and activation of ERK1/2, Akt, and mTOR have been reported in a high percentage of tumors.<sup>5</sup> The activity of clinical inhibitors against RTK activation has been tested in the single largest Phase II study in chordoma to date.<sup>12,30</sup> In this single-arm study, patients with PDGFRB or PDGFB expressing chordoma were treated with imatinib and analyzed at 6 months. While treatment did not lead to significant reduction in tumor burden, it appeared to have a modest antitumor activity in a subset of patients. As all tumors expressed PDGFRB/

Abbreviations used in this paper: IL-2R $\gamma$  = interleukin-2 receptor gamma; NSG = NOD-SCID IL-2R $\gamma$  null; RTK = receptor tyrosine kinase.

PDGFB, this study may highlight the need for inhibitors of downstream signaling pathways in chordoma.

Aberrant activity in the mTOR pathway is one such promising target for chordoma.<sup>23</sup> In children, chordomas have been associated with tuberous sclerosis complex,<sup>1,13</sup> a disease for which mTOR inhibitors have significant benefit.<sup>6</sup> In the more common setting of sporadic disease, mTOR activation has also been observed, suggesting that mTOR inhibition may have utility in a wide spectrum of chordomas.<sup>9</sup> Chordomas can also exhibit loss or reduced expression of tumor suppressor genes,<sup>4,8,17,28,33</sup> many of which are known to regulate PI3K and Akt signaling, such as *PTEN* and tumor suppressor *fragile histidine triad*. Based on these data, advanced chordoma patients with disease resistant to imatinib have been treated with the mTOR inhibitor Sirolimus (rapamycin) with modest overall effect.<sup>31</sup> To date, no studies have examined the activity of the more potent ATP-competitive mTOR inhibitors in preclinical models of this disease.

Despite advances in our understanding of the molecular alterations in chordoma, the treatment options for patients, particularly in the setting of recurrent or metastatic disease, are still inadequate. In particular, for a rare disease like chordoma with few patients, robust preclinical models will be necessary to compare and evaluate treatments that may be impossible to do in standard clinical trials. Importantly, multiple models that reflect the diversity of human disease are critical. In an effort to establish clinically relevant murine models for recurrent disease, we have begun xenografting chordoma tumor samples. The patient-derived xenograft model we employ allows us to examine tumors that faithfully recapitulate the morphology, histology, and cell signaling of human chordoma. In this study, we sought to establish and validate xenograft SF8894 as a clinically relevant model system to study recurrent clival chordoma. In addition, we sought to demonstrate robust activity of the PI3K/Akt/mTOR signaling pathway in recurrent clival chordoma and to suggest that inhibition of mTOR signaling with the ATP-competitive mTOR inhibitor MLN0128 may be a useful therapeutic strategy.

## Methods

### Study Approval

All procedures were performed according to protocols approved by the University of California Committee on Research. Deidentified human chordoma samples were obtained from the UCSF Brain Tumor Research Center Tissue Bank. All experiments involving mice were performed in accordance with protocols approved by the UCSF Institutional Animal Care and Use Committee.

### Establishment of Chordoma Xenograft

The tumor specimen was obtained in the operating room and transported in ice-cold serum-free RPMI 1640 (Life Technologies Corporation). The tumor tissue was minced with a scalpel and an approximately 8-mm<sup>3</sup> piece of tissue was implanted subcutaneously into each flank of 2 NOD-SCID interleukin-2 receptor gamma (IL-2R $\gamma$ ) null (NSG) mice (Jackson Laboratory). The mice were

monitored weekly for evidence of tumor development. Once palpable, the tumor was measured periodically. After 16–20 weeks and at approximately 500 mm<sup>3</sup>, the tumor tissue was isolated, minced, and passaged serially in mice to maintain the tumor as a xenograft. A small portion of the tumor was flash frozen for proteomic analysis and a small portion was fixed in 4% paraformaldehyde for histopathological analysis.

### Histological and Immunohistological Analyses

Deidentified formalin-fixed paraffin-embedded tumor tissue was obtained from the UCSF Brain Tumor Research Center Tissue Bank. Tumor tissue from mice for paraffin embedding and histological and immunohistological analyses was fixed overnight in 4% paraformaldehyde, rinsed in phosphate-buffered saline, and stored in 70% ethanol until further processing. Histological analysis of tumor tissue was performed on H & E stained sections.

Immunohistochemistry was performed as described previously on Benchmark XT (Ventana Medical Systems) using the Ultraview (multimer) detection system.<sup>16,18</sup> The following antibodies were used: p-S6 ribosomal protein (Ser235/236; Cell Signaling no. 2211; 1:200); p-S6 ribosomal protein (Ser240/244; Cell Signaling no. 2215; 1:200); p-4E-BP1 (Thr37/46; Cell Signaling no. 2855; rabbit, 1:400); EGFR (3C6) (Ventana Medical Systems no. 790-2988; 1:1); p-Erk1/2 (Thr202, Tyr204; Invitrogen Corporation no. 18-2389; 1:200); p-PRAS40 (Thr246) (Cell Signaling no. 2997; 1:25); PTEN (138G6) (Cell Signaling no. 9559; 1:100); p-Akt (Ser473; Cell Signaling no. 4060; 1:100); MIB-1 (30-9) (Ventana Medical Systems anti-Ki-67 no. 790-4286; undiluted).

### Drug Treatment of Subcutaneous Chordoma Xenografts

MLN0128 was synthesized as previously described.<sup>10</sup> Mice harboring subcutaneous chordoma xenografts were treated daily with MLN0128 (1 mg/kg dissolved in 1% *N*-methyl-2-pyrrolidone, 15% polyvinylpyrrolidone, 84% water) or saline for 4 days. Three hours after the final dose tumors were harvested. A portion was flash frozen in liquid nitrogen and another portion was fixed for paraffin embedding, as described above. A total of 3 subcutaneous flank tumors were analyzed from 2 mice for each condition.

### Luminex xMAP

Tumor tissue from mice was collected at the time the mice were euthanized and flash frozen in liquid nitrogen. As recommended by the manufacturer (EMD Millipore Corporation), protein lysate (25  $\mu$ g) was incubated with MILLIPLEX MAP Akt/mTOR phosphoprotein magnetic and total protein bead-based multianalyte panels (48-612MAG and 48-611MAG) and the non-magnetic GAPDH analyte (46-667). Samples were analyzed using Bio-Plex 200 (Bio-Rad Laboratories, Inc.).

## Results

### Clinical Presentation and Pathological Confirmation of Chordoma

A 56-year-old man first presented in 2006 with dys-

## Generation of a patient-derived chordoma xenograft

phagia, weight loss, and development of a lisp. Magnetic resonance imaging revealed an 8-cm midline lesion centered on the clivus, encasing and laterally displacing the carotid arteries bilaterally and extending below the odontoid (Fig. 1A and B). In March 2007, the lesion was resected by an endoscopic transsphenoidal approach, and a pathological diagnosis of chordoma was made (Fig. 2A). Follow-up imaging in May 2007 demonstrated tumor growth in soft tissues surrounding the clivus, destruction of C1–2, and evidence of occipitocervical instability (Fig. 1C and D). Staged operations were performed to decompress the upper cervical spine with posterior occiput–C5 fusion followed by transmandibular C1–2 decompression and chordoma excision. The patient subsequently underwent proton-beam irradiation in August 2007. In September 2011, the patient developed acute onset of leg weakness and left hand numbness. Magnetic resonance imaging demonstrated a tumor extending from C-5 to T-2, cord compression myelopathy, and partial erosion of the T-1 and T-2 vertebral bodies (Fig. 1E and F). The patient underwent posterior cervical and thoracic fu-

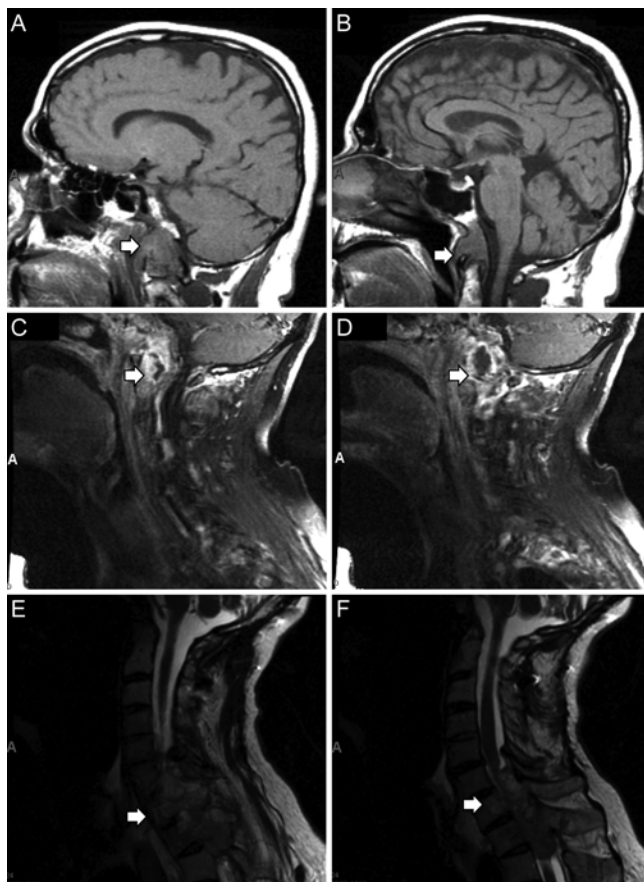


**Fig. 1.** Sagittal MRI of primary clival chordoma and recurrent tumor involving the cervical and thoracic spine. **A and B:** T1-weighted images of brain demonstrating clival mass extending to inferior portion of odontoid (arrows), obtained in January 2007. **C and D:** T1-weighted cervical images demonstrating destructive lesion in soft tissues of skull base and upper cervical spine (arrows), obtained in May 2007. **E and F:** T2-weighted cervical images demonstrating extension of tumor from C-5 to T-2 with severe cord compression (arrows), obtained in September 2011.

sion extending to T-3, including C6–7 and T1–2 laminectomies and left-side T-1 transpedicular corpectomy and T-2 costotransversectomy, for removal of the epidural tumor. Analysis of tumor tissue from each excision demonstrated histopathological features of chordoma (Fig. 2A and B). Tumors had an overall lobulated appearance with tumor cells separated by fibrous septa. The tumor cells contained small round nuclei and often had abundant cytoplasm with large cytoplasmic vacuolations (physaliferous cells). Immunohistochemistry confirmed the diagnosis of chordoma with strong diffuse immunopositivity for brachyury and pan-cytokeratin (AE1/3 and CAM5.2) (Fig. 2A and B).

### *Establishment and Characterization of a Chordoma Xenograft From a Recurrent Clival Tumor*

Tumor tissue from the recurrent T-2 lesion (recurrence no. 2) was obtained intraoperatively and implanted subcutaneously into NSG mice. Mice were monitored over 170 days and successful xenograft growth was detected by 90 days postimplantation. Two of 4 tumor fragments grew and were harvested at 16 and 20 weeks postimplantation for passage into additional recipient mice. SF8894 tumors were maintained as xenografts through serial passage. Histological and immunohistological analyses of the recurrent clival chordoma and the chordoma xenograft SF8894 demonstrated striking similarity (Fig. 2B and C). Similar to the human tumor, the xenograft grew as a lobulated mass composed of tumor cells with small round nuclei and cytoplasm with abundant vacuolations, and immunohistochemistry demonstrated diffuse nuclear positivity for brachyury and cytoplasmic positivity for cytokeratin (Fig. 2C).

### *Activation of the PI3K/Akt/mTOR Signaling Pathway in Chordoma*

Abnormal activation of the PI3K/Akt/mTOR signaling pathway has been reported in a significant subset of chordoma.<sup>23</sup> To investigate the activity of this pathway in chordoma and to determine if xenograft SF8894 mimicked these alterations, we analyzed the tumors using phospho-specific immunohistochemistry (Fig. 2D–H). Immunostaining for p-S6 (Ser240/244) and p-Erk1/2 (Thr202, Tyr204) demonstrated a nearly identical pattern of strong diffuse immunopositivity in the primary clival chordoma, the recurrent tumor, and the xenograft. Additional immunostaining for p-Akt (Ser473), p-PRAS40 (Thr246), p-4EBP1 (Thr37/46), and p-S6 (Ser235/236) confirmed the strong and very similar pattern of immunopositivity in both the recurrent tumor and the xenograft. Immunopositivity was primarily cytoplasmic for p-Akt, p-PRAS40, and p-S6 and was both nuclear and cytoplasmic for p-4EBP1 and p-Erk1/2, similar to previous reports.<sup>26</sup> In the primary recurrent and xenograft clival chordoma, both EGFR expression and PTEN expression were negative (Fig. 2D–F).

### *Inhibition of mTOR Signaling Activity in Chordoma Xenografts*

Having demonstrated a similar pattern of PI3K/Akt/

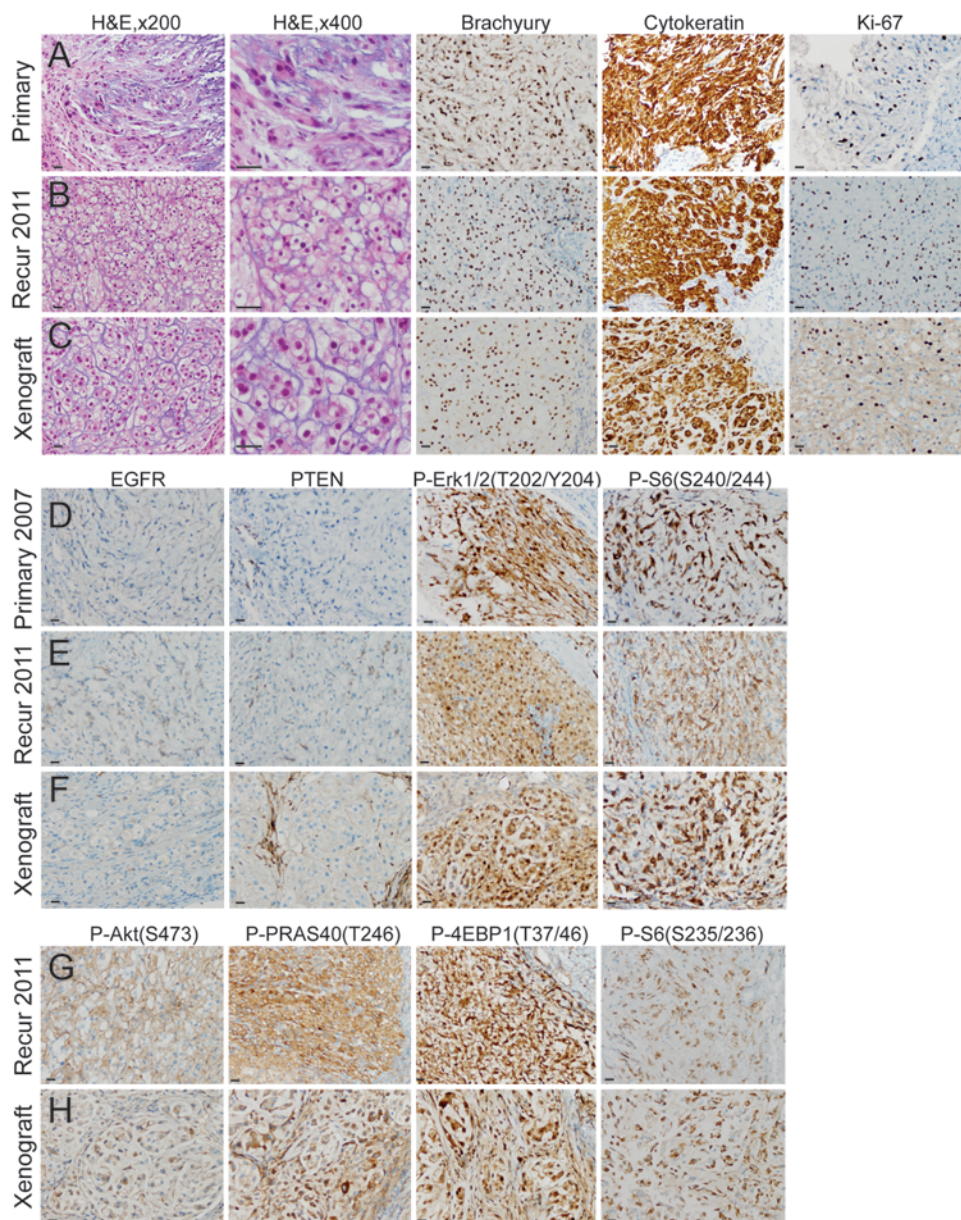


**Fig. 2.** Chordoma xenograft SF8894 recapitulates histological and immunohistological features of the resected chordoma including activation of the PI3K/Akt/mTOR pathway. The primary clival tumor resected in 2007 (**A and D**), the recurrent (Recur) tumor in 2011 (**B, E, and G**), and the xenograft derived from the recurrent tumor (**C, F, and H**) had similar histopathological and immunohistopathological features characteristic of chordoma. H & E staining demonstrated tumor cells with bland small nuclei and abundant vacuolated cytoplasm. Immunohistochemistry demonstrated robust nuclear brachyury expression, cytoplasmic cytokeratin positivity, and scattered Ki-67 positive proliferating tumor cells. The clival tumor (**D**), the recurrent tumor (**E**), and the tumor xenograft (**F**) had a similar profile using a panel of immunomarkers including phospho-specific antibodies. All 3 had abundant levels of phosphorylated S6 (S240/244) and Erk1/2 (T202, Y204). Using an extended panel of phospho-specific antibodies on the recurrent tumor and the xenograft, abundant levels of phosphorylated Akt (S473), PRAS40 (T246), 4EBP1 (T37/46), and S6 (S235/236) were identified. EGFR and PTEN immunostaining was negative in tumor cells. Bars = 30  $\mu$ m.

mTOR signaling pathway activity in recurrent clival chordoma and the derived chordoma xenograft, we used the xenograft as an *in vivo* model to determine whether an mTOR kinase (mTORC1/mTORC2) inhibitor might decrease mTOR pathway activity in tumors. Mice harboring subcutaneous chordoma xenografts were treated daily with MLN0128, an ATP-competitive inhibitor of mTOR, or saline for 4 days. Three hours after the final dose, tumors were harvested and subjected to phosphoproteome profil-

ing using Luminex technology (Luminex Corporation) and phospho-specific immunohistochemistry (Fig. 3). Following treatment, there was a statistically significant reduction in phospho-mTOR (Ser2448) ( $p = 0.019$ ,  $n = 3$  tumors each treatment) and there was a trend for decreased p-S6 (Ser235/236) levels compared to saline-treated control mice. According to phospho-specific immunohistochemistry, the MLN0128-treated tumors had decreased p-S6 (Ser240/244) levels compared to the saline-treated tumors.

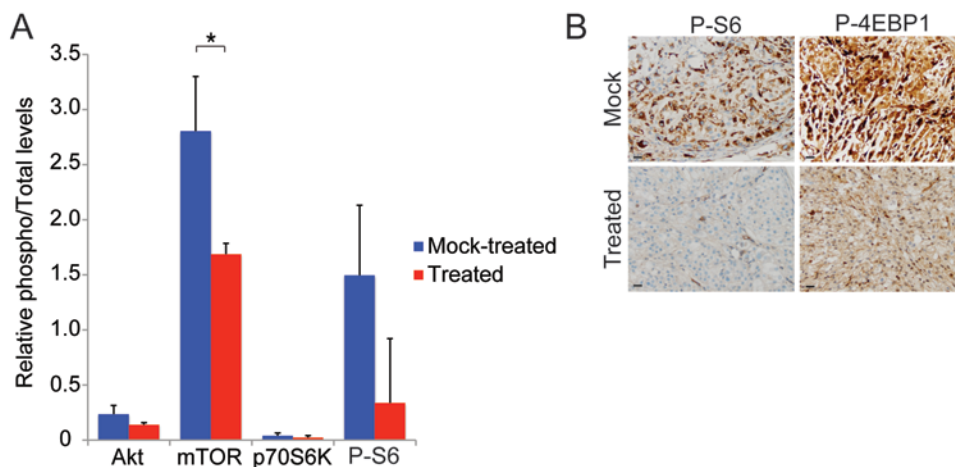


**Fig. 3.** Phosphoproteome profiling of xenografts from mice treated with ATP-site mTOR inhibitors. **A:** Following daily treatment with MLN0128 or mock treatment with saline for 4 days, tumors were harvested and protein lysate was subjected to phosphoproteome profiling using Luminex technology in duplicate. MLN0128-treated tumors exhibited a significant reduction in phosphorylation of mTOR (S2448) compared to tumors from saline-treated control mice (\**p* = 0.019, *n* = 3 tumors for each treatment). **B:** Representative images of MLN0128- and mock-treated tumors immunostained for p-S6 (S240/244). Bars = 30  $\mu$ m.

### Discussion

Despite aggressive surgical intervention and radiation treatment of chordoma, tumor recurrence is common, and novel therapeutic strategies are needed. In this study, we report on the establishment and characterization of a primary chordoma xenograft from a recurrent clival chordoma. We demonstrate that the chordoma xenograft recapitulates the histopathological features and signaling pathway activity of the primary tumor, and we provide preliminary data that this xenograft model will be useful as a preclinical therapeutic model for recurrent chordoma.

The establishment of primary chordoma cell lines and xenografts is critical for advances in our understanding of the biology of this disease and its treatment. There are now several chordoma cell lines that have been established,<sup>3,11,14,20,21,25,27,35</sup> but few can be xenografted into mice.<sup>14,24</sup> With the establishment of SF8499, there are now 2 primary chordoma xenografts available for study.<sup>29</sup>

Activity of the mTOR signaling pathway, a critical regulator of protein synthesis and entry into the G1 phase of the cell cycle, is frequently altered in chordoma.<sup>23</sup> Cellular mTOR exists in 2 different complexes, mTOR Complex 1 (mTORC1) and mTOR Complex 2 (mTORC2). Although rapamycin and its derivatives partially inhibit mTOR in mTORC1, they do not inhibit mTOR in mTORC2. MLN0128 is an ATP-competitive inhibitor of mTOR that acts as a dual mTORC1/2 inhibitor, and it has shown promising results in tumor models of prostate cancer, breast cancer, and multiple myeloma.<sup>7,10,15</sup> Our data argue for preclinical testing of dual mTORC1/2 inhibitors in chordoma and suggest inhibition of mTOR signaling may be a promising therapeutic strategy in chordoma.

### Conclusions

These data demonstrate that SF8894 is a clinically relevant model for preclinical therapeutic testing in chordoma and suggest that additional preclinical studies of

mTOR inhibitors for the therapeutic targeting of chordoma are needed.

### Acknowledgments

We would like to thank the patients who have allowed their tumor tissues to be studied, the Chordoma Foundation, and Josh Sommer. Special thanks to Mi Zhou for helpful technical advice and Joseph L. Wiemels and John K. Wiencke for use of their Bio-Plex 200.

### Disclosure

Dr. Mummaneni receives honoraria and royalties from DePuy Spine; honoraria from Globus; royalties from Thieme Publishers; and royalties from Quality Medical Publishers.

This work was supported in part by the National Institutes of Health (grant no. R01 NS081117 to J.J.P.), the Waxman Foundation (K.M.S.), and the UCSF Brain Tumor SPORE (grant no. CA097257 to C.C.).

Author contributions to the study and manuscript preparation include the following. Conception and design: Phillips, Cowdrey, Shokat, Bollen, Hann. Acquisition of data: Phillips, Robinson, Cowdrey, Mummaneni, Ducker, Hann. Analysis and interpretation of data: Phillips, Davies, Shokat, Bollen, Hann. Drafting the article: Phillips. Critically revising the article: all authors. Reviewed submitted version of manuscript: all authors. Approved the final version of the manuscript on behalf of all authors: Phillips. Statistical analysis: Phillips. Administrative/technical/material support: Phillips. Study supervision: Hann.

### References

- Börgel J, Olschewski H, Reuter T, Miterski B, Epplen JT: Does the tuberous sclerosis complex include clivus chordoma? A case report. *Eur J Pediatr* **160**:138, 2001
- Catton C, O'Sullivan B, Bell R, Laperriere N, Cummings B, Fornasier V, et al: Chordoma: long-term follow-up after radical photon irradiation. *Radiother Oncol* **41**:67-72, 1996
- DeComas AM, Penfornis P, Harris MR, Meyer MS, Pochampally RR: Derivation and characterization of an extra-axial chordoma cell line (EACH-1) from a scapular tumor. *J Bone Joint Surg Am* **92**:1231-1240, 2010

4. Diaz RJ, Guduk M, Romagnuolo R, Smith CA, Northcott P, Shih D, et al: High-resolution whole-genome analysis of skull base chordomas implicates FHIT loss in chordoma pathogenesis. **Neoplasia** **14**:788–798, 2012
5. Fasig JH, Dupont WD, LaFleur BJ, Olson SJ, Cates JM: Immunohistochemical analysis of receptor tyrosine kinase signal transduction activity in chordoma. **Neuropathol Appl Neurobiol** **34**:95–104, 2008
6. Franz DN, Belousova E, Sparagana S, Bebin EM, Frost M, Kuperman R, et al: Efficacy and safety of everolimus for subependymal giant cell astrocytomas associated with tuberous sclerosis complex (EXIST-1): a multicentre, randomised, placebo-controlled phase 3 trial. **Lancet** **381**:125–132, 2013 (Erratum in **Lancet** **381**:116, 2013)
7. García-García C, Ibrahim YH, Serra V, Calvo MT, Guzmán M, Grueso J, et al: Dual mTORC1/2 and HER2 blockade results in antitumor activity in preclinical models of breast cancer resistant to anti-HER2 therapy. **Clin Cancer Res** **18**:2603–2612, 2012
8. Hallor KH, Staaf J, Jönsson G, Heidenblad M, Vult von Steyern F, Bauer HC, et al: Frequent deletion of the CDKN2A locus in chordoma: analysis of chromosomal imbalances using array comparative genomic hybridisation. **Br J Cancer** **98**:434–442, 2008
9. Han S, Polizzano C, Nielsen GP, Hornicek FJ, Rosenberg AE, Ramesh V: Aberrant hyperactivation of akt and mammalian target of rapamycin complex 1 signaling in sporadic chordomas. **Clin Cancer Res** **15**:1940–1946, 2009
10. Hsieh AC, Liu Y, Edlind MP, Ingolia NT, Janes MR, Sher A, et al: The translational landscape of mTOR signalling steers cancer initiation and metastasis. **Nature** **485**:55–61, 2012
11. Hsu W, Mohyeldin A, Shah SR, ap Rhys CM, Johnson LF, Sedora-Roman NI, et al: Generation of chordoma cell line JHC7 and the identification of Brachyury as a novel molecular target. Laboratory investigation. **J Neurosurg** **115**:760–769, 2011
12. Launay SG, Chetaille B, Medina F, Perrot D, Nazarian S, Guiramand J, et al: Efficacy of epidermal growth factor receptor targeting in advanced chordoma: case report and literature review. **BMC Cancer** **11**:423, 2011
13. Lee-Jones L, Aligianis I, Davies PA, Puga A, Farndon PA, Stemmer-Rachamimov A, et al: Sacrococcygeal chordomas in patients with tuberous sclerosis complex show somatic loss of TSC1 or TSC2. **Genes Chromosomes Cancer** **41**:80–85, 2004
14. Liu X, Nielsen GP, Rosenberg AE, Waterman PR, Yang W, Choy E, et al: Establishment and characterization of a novel chordoma cell line: CH22. **J Orthop Res** **30**:1666–1673, 2012
15. Maiso P, Liu Y, Morgan B, Azab AK, Ren P, Martin MB, et al: Defining the role of TORC1/2 in multiple myeloma. **Blood** **118**:6860–6870, 2011
16. McBride SM, Perez DA, Polley MY, Vandenberg SR, Smith JS, Zheng S, et al: Activation of PI3K/mTOR pathway occurs in most adult low-grade gliomas and predicts patient survival. **J Neurooncol** **97**:33–40, 2010
17. Mobley BC, McKenney JK, Bangs CD, Callahan K, Yeom KW, Schneppenheim R, et al: Loss of SMARCB1/INI1 expression in poorly differentiated chordomas. **Acta Neuropathol** **120**:745–753, 2010
18. Mueller S, Phillips J, Onar-Thomas A, Romero E, Zheng S, Wiencke JK, et al: PTEN promoter methylation and activation of the PI3K/Akt/mTOR pathway in pediatric gliomas and influence on clinical outcome. **Neuro Oncol** **14**:1146–1152, 2012
19. Naka T, Iwamoto Y, Shinohara N, Ushijima M, Chuman H, Tsuneyoshi M: Expression of c-met proto-oncogene product (c-MET) in benign and malignant bone tumors. **Mod Pathol** **10**:832–838, 1997
20. Ostroumov E, Hunter CJ: Identifying mechanisms for therapeutic intervention in chordoma: c-Met oncoprotein. **Spine (Phila Pa 1976)** **33**:2774–2780, 2008
21. Ostroumov E, Hunter CJ: The role of extracellular factors in human metastatic chordoma cell growth in vitro. **Spine (Phila Pa 1976)** **32**:2957–2964, 2007
22. Park L, Delaney TF, Liebsch NJ, Hornicek FJ, Goldberg S, Mankin H, et al: Sacral chordomas: impact of high-dose proton/photon-beam radiation therapy combined with or without surgery for primary versus recurrent tumor. **Int J Radiat Oncol Biol Phys** **65**:1514–1521, 2006
23. Presneau N, Shalaby A, Idowu B, Gikas P, Cannon SR, Gout I, et al: Potential therapeutic targets for chordoma: PI3K/AKT/TSC1/TSC2/mTOR pathway. **Br J Cancer** **100**:1406–1414, 2009
24. Presneau N, Shalaby A, Ye H, Pillay N, Halai D, Idowu B, et al: Role of the transcription factor T (brachyury) in the pathogenesis of sporadic chordoma: a genetic and functional-based study. **J Pathol** **223**:327–335, 2011
25. Ricci-Vitiani L, Pierconti F, Falchetti ML, Petrucci G, Maira G, De Maria R, et al: Establishing tumor cell lines from aggressive telomerase-positive chordomas of the skull base. Technical note. **J Neurosurg** **105**:482–484, 2006
26. Rojo F, Najera L, Lirola J, Jiménez J, Guzmán M, Sabadell MD, et al: 4E-binding protein 1, a cell signaling hallmark in breast cancer that correlates with pathologic grade and prognosis. **Clin Cancer Res** **13**:81–89, 2007
27. Scheil S, Brüderlein S, Liehr T, Starke H, Herms J, Schulte M, et al: Genome-wide analysis of sixteen chordomas by comparative genomic hybridization and cytogenetics of the first human chordoma cell line, U-CH1. **Genes Chromosomes Cancer** **32**:203–211, 2001
28. Shalaby A, Presneau N, Ye H, Halai D, Berisha F, Idowu B, et al: The role of epidermal growth factor receptor in chordoma pathogenesis: a potential therapeutic target. **J Pathol** **223**:336–346, 2011
29. Siu IM, Salmasi V, Orr BA, Zhao Q, Binder ZA, Tran C, et al: Establishment and characterization of a primary human chordoma xenograft model. Laboratory investigation. **J Neurosurg** **116**:801–809, 2012
30. Stacchiotti S, Longhi A, Ferraresi V, Grignani G, Comandone A, Stupp R, et al: Phase II study of imatinib in advanced chordoma. **J Clin Oncol** **30**:914–920, 2012
31. Stacchiotti S, Marrari A, Tamborini E, Palassini E, Viridis E, Messina A, et al: Response to imatinib plus sirolimus in advanced chordoma. **Ann Oncol** **20**:1886–1894, 2009
32. Tamborini E, Miselli F, Negri T, Lagonigro MS, Staurengo S, Dagrada GP, et al: Molecular and biochemical analyses of platelet-derived growth factor receptor (PDGFR) B, PDGFRA, and KIT receptors in chordomas. **Clin Cancer Res** **12**:6920–6928, 2006
33. Tamborini E, Viridis E, Negri T, Orsenigo M, Brich S, Conca E, et al: Analysis of receptor tyrosine kinases (RTKs) and downstream pathways in chordomas. **Neuro Oncol** **12**:776–789, 2010
34. Weinberger PM, Yu Z, Kowalski D, Joe J, Manger P, Psyrra A, et al: Differential expression of epidermal growth factor receptor, c-Met, and HER2/neu in chordoma compared with 17 other malignancies. **Arch Otolaryngol Head Neck Surg** **131**:707–711, 2005
35. Yang C, Hornicek FJ, Wood KB, Schwab JH, Choy E, Iafrate J, et al: Characterization and analysis of human chordoma cell lines. **Spine (Phila Pa 1976)** **35**:1257–1264, 2010

Manuscript submitted March 24, 2013.

Accepted October 10, 2013.

Please include this information when citing this paper: published online November 29, 2013; DOI: 10.3171/2013.10.JNS13598.

Address correspondence to: Joanna J. Phillips, M.D., Ph.D., 1450 Third St., HD281, Box 0520, Helen Diller Family Cancer Research Bldg., San Francisco, CA 94158. email: joanna.phillips@ucsf.edu.